



CORRIGENDUM TO:

**SIMULATION OF ADSORPTION PROCESS IN A ROTARY SOLID DESICCANT
WHEEL**

Alia Sofia Norazam¹, Haslinda Mohamed Kamar^{1*}, Nazri Kamsah¹, Muhamad Idrus Alhamid²

¹*Faculty of Mechanical Engineering, Universiti Teknologi Malaysia, 81310 UTM Skudai, Johor,
Malaysia*

²*Department of Mechanical Engineering, Faculty of Engineering, Universitas Indonesia, Kampus UI
Depok, Depok 16424, Indonesia*

In Title, typed as:

“Simulation of Adsorption Process in a Rotary Solid Desiccant Wheel”

The Title should be written as follows:

“Performance Analysis of a Solid Desiccant Wheel Material”

SIMULATION OF ADSORPTION PROCESS IN A ROTARY SOLID DESICCANT WHEEL

Alia Sofia Norazam¹, Haslinda Mohamed Kamar^{1*}, Nazri Kamsah¹, Muhamad Idrus Alhamid²

¹*Faculty of Mechanical Engineering, Universiti Teknologi Malaysia, 81310 UTM Skudai, Johor, Malaysia*

²*Department of Mechanical Engineering, Faculty of Engineering, Universitas Indonesia, Kampus UI Depok, Depok 16424, Indonesia*

(Received: August 2019 / Revised: October 2019 / Accepted: October 2019)

ABSTRACT

Solid desiccant air dehumidifier systems are widely used to supply dry air for many industrial processes. As humid atmospheric air flows through the system, the water vapor in the air is adsorbed by the desiccant material, resulting in dry air leaving the system. A numerical solution has become the preferred choice for determining the performance criteria of desiccant materials. The aim of this study is to determine the moisture removal capacity (MRC), dehumidification effectiveness (ϵ_{DW}), and thermal effectiveness (ϵ_{th}) of a solid desiccant wheel material using a numerical method. A representative three-dimensional model of an air channel enclosed with desiccant material was developed and meshed using triangular elements. Flow simulations were carried out under a transient condition. The model was validated by comparing the simulation results for moisture content and air temperature at the outlet of the air channel with similar results using experimental data obtained from the literature. The relative errors for the desorption process were found to be 0.14% for air temperature and 3.7% for air humidity. For the adsorption process, they were around 3.2 and 0.01%, respectively. These figures indicate that the numerical model has an excellent ability to estimate the desiccant material performance. It was also found that at any given regeneration temperature, silica gel-CaCl₂ has the highest MRC, dehumidification effectiveness, and thermal effectiveness compared to silica gel B and Zeolite 13X.

Keywords: Air dehumidifier; Computational fluid dynamics (CFD); Solid desiccant; Transient flow simulation

1. INTRODUCTION

Specific humidity or moisture content is the actual mass of water vapor in 1 kg of dry air. Whereas relative humidity is the ratio of the actual mass of moisture in the air at a given temperature to the maximum amount of moisture that air can hold at the same temperature. Relative humidity and dry-bulb temperature are two parameters used to indicate the level of personal comfort. People commonly focus only on temperature but rarely on moisture; however, the high relative humidity of indoor air may have serious health implications for occupants. This is because, during the perspiration process, surrounding air that has a relative humidity close to 100% is unable to absorb the latent heat released by the human body. Sustained periods under these conditions can lead to people feeling thermally uncomfortable due to an increase in body temperature and can

*Corresponding author's email: haslinda@mail.fkm.utm.my, Tel. +607-5534748, Fax: +607-5557097
Permalink/DOI: <https://dx.doi.org/10.14716/ijtech.v10i6.3590>

trigger dehydration and heatstroke. The effect citrus of this can result in respiratory and skin problems. Besides that, it can also create a humid environment conducive to the growth of bacteria (Satwikasari et al., 2018; Tharim et al., 2018). Therefore, it is necessary to control the humidity level in the air in order to ensure personal comfort in a confined space.

Malaysia is a tropical country, characterized by high daytime temperatures of 29–34°C and relative humidity of 70–90% throughout the year (Makaremi et al., 2012). The recommended temperature and relative humidity for the indoor environment are 23–26°C and 30–60%, respectively, as set out by ASHRAE Standard 55 (Yang & Zhang, 2008). In order to meet the ASHRAE requirement, air-conditioning systems are widely used in Malaysia. The number of air-conditioning systems in use has increased from 13,000 units in 1970 to more than 250,000 units in 1991, with the number expected to rise to around 1.5 million units by 2020 (Daou et al., 2006). However, the growing demand for air-conditioning has contributed to the massive consumption of electrical power. Other than sensible cooling, air-conditioning also performs the essential task of humidity control. In conventional air-conditioning units, the cooling process and air dehumidification are generally driven by a cooling coil (Nguyen & Aiello, 2013). The high humidity in Malaysia results in a significantly high air dehumidification load. The conventional method consumes a large amount of electricity as a result of the overcooling process to achieve lower humidity. Modern air-conditioning has recently included separate handling of the dehumidification load and sensible cooling capacity, which reduces its power requirement. This is usually integrated with the air-conditioning system to provide comfort inside buildings such as residential houses and offices, which require around 60–70% humidity, and hospital operating rooms, which need around 50–60% humidity (Sookchaiya et al., 2010).

A dehumidifier is a device that can be used to reduce the humidity of the air. Some industries, such as textile, foods, pharmaceutical, and battery production, are susceptible to moisture. These industries require an environment with low humidity within the range of 20–55% in order to maintain the quality of their products and machines (Kamar et al., 2016). Humid surrounding air will lead to the corrosion of metals, deteriorated characteristics of hygroscopic material, and increased harmful activity of micro-organisms in products (Moncmanová, 2007). The system has two different features, i.e., compressor-based (CBD) and desiccant-based dehumidifiers. CBD is a conventional method of removing water vapor by condensation based on the vapor compression refrigeration system (Rambhad et al., 2016). Humid air passes through a cooling coil where it is cooled below its dewpoint temperature in order for condensation to occur. However, the CBD system consumes large amounts of electrical energy during the cooling process. The desiccant dehumidification system, meanwhile, has received much recent attention as an alternative to the CBD type (Yamaguchi & Saito, 2013). Here, air is dehumidified without condensation, using only sorption from desiccant material instead. This can help reduce the electrical energy consumption of the CBD system.

Desiccant dehumidifiers can be characterized into two categories, i.e., liquid desiccant dehumidifier (LDD) and solid desiccant dehumidifier (SDD). The main components in an LDD system are the absorber and regenerator. Both parts are filled with constructed packing materials to enhance the contact area between the desiccant solution and process air. The absorber is concentrated with a desiccant solution to enable it to absorb water vapor from the process air. The process air, driven by a fan, flows in an upward direction within the liquid desiccant. Then, the dilute liquid desiccant flows out of the absorber and is pumped to the regenerator. In the regenerator, ambient air at a high air temperature flows in an upward direction within the diluted liquid desiccant. The ambient air absorbs the water vapor from the diluted liquid desiccant due to the difference in vapor pressure between the liquid desiccant and the air. The regenerator restores the ability of the liquid desiccant to absorb moisture for the next process cycle. The advantage of the liquid desiccant is that regeneration can be carried out at a lower temperature

with high moisture removal capacity (MRC) (Misha et al., 2012). However, this can lead to corrosion of the dehumidifier components.

An SDD consists of a desiccant material constructed in the form of a wheel that rotates at a low speed, an air heater, and a drive motor. The wheel comprises a process air section and a regeneration air section. The humid process (ambient) air flows through the process air section, during which time the desiccant material adsorbs moisture from the air. The temperature of the air increases slightly since the adsorption process releases heat. As a result, the process air leaves the desiccant wheel with lower humidity and a somewhat higher temperature. On the other hand, hot regeneration air flows through the regeneration section of the wheel in the opposite direction to the process air. As this happens, the water vapor sitting on the desiccant material surface is desorbed by the hot air. This desorption process also involves heat transfer, and as a result, the regeneration air exits the wheel with higher humidity and a slightly lower temperature. The regeneration section of the desiccant wheel then becomes dry, ready for the new process air to flow through it. Since the desiccant wheel is rotating slowly, the above sequences of processes are continuous. This system consumes less electrical energy due to the lack of pump usage and moving parts (Wu & Wang, 2006). It is also more straightforward than liquid desiccants (Misha et al., 2012) because it has a low risk of crystallization and only a slight risk of damage due to high temperatures. Also, the solid desiccant material is environmentally friendly.

Two of the most critical components in the SDD system are the desiccant wheel and solid desiccant material itself, which is corrugated in the numerous channels inside the rotary wheel. Cheng et al. (2016) carried out a study on the influence of desiccant material properties on dehumidification effectiveness and showed that it is influenced by the thermal conductivity, specific heat, porosity, tortuosity, and thickness of desiccant materials. Jia et al. (2007) compared the effect of silica gel and composite materials on the coefficient of performance (COP) and MRC. It was found that the composite desiccant wheel adsorbed more moisture than the conventional one. Zhang et al. (2014) investigated the effects of ten types of desiccant materials on COP, specific dehumidification power (SDP), and dehumidification efficiency. The performance of the desiccant wheel is affected by several parameters, including wheel geometry, rotation wheel speed, inlet process air properties, inlet regeneration temperature, and velocity (Yamaguchi & Saito, 2013; Cheng et al. 2016). Jia et al. (2007) conducted a similar study using an experimental method. Others used a numerical method as an alternative to the experiment (Misha et al., 2012). This approach is less complicated, much cheaper, less time-consuming, and less laborious. Cheng et al. (2016) established a three-dimensional (3D) single-channel model representing desiccant material and found the model to be essential in obtaining accurate predictions. For simplification, many researchers have used a single-channel model to describe the airflow through the desiccant wheel. This may be for reasons of geometric similarity and in order to avoid prohibitive computation costs, and it is reasonable to use a single channel to represent the multiple channels in the desiccant wheel (Yadav et al., 2014).

Recent research and developments of SDD have focused on improving energy efficiency by using a low-grade heat source such as solar energy so that the regeneration temperature can be reduced. The regeneration temperature is determined by the properties of desiccant material, which should have high adsorption capacity and good regeneration ability. Though some novel materials have improved the performances of SDD systems, no material currently available can perfectly satisfy the entire demand for an energy-efficient, environmentally friendly, and affordable material. Therefore, more studies on the development of desiccant materials are needed in order to meet the requirements of industry. Traditionally, these have involved conducting experiments on the SDD system. However, a series of tests have needed to be performed as part of the experiments and clearly, due to the need to install a variety of desiccant wheel models, this practice is highly costly and time-consuming. In order to ensure efficiency in carrying out the parametric analysis,

numerical modeling should be used where it can promote energy and cost-saving. There are still only limited studies in three-dimensional (3D) modeling representing solid desiccant material, where major past researchers have only developed simplified models in 1D or 2D. These models reduce the validity of simplified models of the SDD. Therefore, this study aims to examine the effects of air regeneration temperature and desiccant material on the performance criteria of solid desiccant material using numerical modeling. A 3D model of a single air channel was developed to represent a flow path of the process and regeneration air through the solid desiccant material. Flow simulations were carried out under a transient state to predict the average temperature and humidity of the process air at the channel exit. The model was validated by comparing the simulation results with experimental data obtained from the literature. The performance criteria considered are MRC, dehumidification effectiveness, and thermal effectiveness. This research produces an economical method for determining the performance criteria of solid desiccant materials. Thus, it could identify the most suitable materials that give the lowest possible humidity of process air at any given regeneration air temperature.

2. ROTARY DESICCANT WHEEL

The solid desiccant wheel of an air dehumidifier system consists of a desiccant material constructed in the form of a wheel that rotates at a low speed, an air heater, and a drive motor. The wheel comprises a process air section and a regeneration air section. The humid process (ambient) air flows through the process air section during which time the desiccant material adsorbs the moisture content of the air. The temperature of this air rises slightly since the adsorption process releases heat energy. As a result, the process air leaves the desiccant wheel with lower humidity and a somewhat higher temperature. In contrast, hot regeneration air flows through the regeneration section of the wheel, usually in the opposite direction to the process air. As this happens, the water vapor sitting on the desiccant material surface is absorbed by the hot air. This absorption process also involves heat transfer, and as a result, the regeneration air exits the wheel with higher humidity and a slightly lower temperature. The regeneration section of the desiccant wheel now becomes dry and is ready for the new process air to flow through it. Since the desiccant wheel rotates slowly, the above sequences of processes are continuous.

3. MODEL OF ADSORPTION PROCESS

A mathematical model of the adsorption process in a 3D air channel geometry was reported by Zhang et al. (2014). The governing equations related to the air comprise the mass and energy conservation equations given as follows:

$$\frac{\partial}{\partial t}(\omega_a) + u \nabla \cdot (\omega_a) = \frac{4k}{D_h}(\omega_{ds} - \omega_a) \quad (1)$$

$$\rho_a c_{pa} \frac{\partial}{\partial t}(T_a) + u \rho_a c_{pa} \nabla \cdot (T_a) = \frac{4h}{D_h}(T_{ds} - T_a) \quad (2)$$

The second term of Equation 1 represents the convection-diffusion process, while the term on the right-hand side represents the transfer of water vapor to the adsorbent layer. The second term of Equation 2 describes a convective heat transfer due to fluid flow, while the term on the right-hand side represents the heat transfer to the adsorbent layer. The convective heat transfer coefficient, h , and the mass transfer coefficient, k , are calculated using Equations 3a and 3b, respectively.

$$h = \frac{Nu k_a}{D_h} \quad (3a)$$

$$k = \frac{Sh D_{va}}{D_h} \quad (3b)$$

The value of Nu and Sh for sinusoidal channel shape are 2.2 and 2.05, respectively (Zhang et al., 2014). The mass conservation and energy balance in the solid desiccant are given by the following Equations 4 and 5, respectively.

$$(1 - \varepsilon)\rho_d \frac{\partial}{\partial t}(\omega_d) + \rho_d \nabla \cdot (-D_{vs} \nabla \omega_d) = -\rho_d k_m(\omega_{eq} - \omega_d) \tag{4}$$

$$\rho_d c_d \frac{\partial}{\partial t}(T_d) + \nabla \cdot (-k_d \nabla T_d) = q_{st} \rho_d k_m(\omega_{eq} - \omega_d) \tag{5}$$

The second term of Equation 4 describes the mass diffusion process that occurs in the solid desiccant. The right-hand term of the equation represents the mass adsorption rate. In Equation 5 the second term describes the heat conduction that occurs in the solid desiccant material, and the term on the right-hand side represents the rate of adsorption heat. The equilibrium water uptake in the desiccant material, ω_{eq} , and the relative humidity, ϕ , at atmospheric condition are given by Equations 6a and 6b, respectively.

$$\omega_{eq} = \frac{f \omega_{max}}{(1 - C + \frac{C}{\phi})} \tag{6a}$$

$$\phi = \omega_d (10^{-6} e^{5295/T_d}) \tag{6b}$$

The boundary conditions at the inlet of the air channel are given by Equations 7a and 7b, while the initial conditions at time $t = 0$ are given by Equations 7c and 7d, as follows:

$$T_a|_{x=0} = T_{a,inlet} \tag{7a} \qquad \omega_a|_{x=0} = \omega_{a,inlet} \tag{7b}$$

$$T_a|_{t=0} = T_{a,ambient} \tag{7c} \qquad \omega_a|_{t=0} = \omega_{a,ambient} \tag{7d}$$

3.1. Numerical Simulation Methodology

Figure 1 (Zhang et al., 2014) shows a simplified geometry of a single air channel in desiccant material for the adsorption and desorption processes. The dimension of the channel length, L , is 100 mm; height, h , is 1.8 mm, and the desiccant thickness, t , is 0.15 mm.

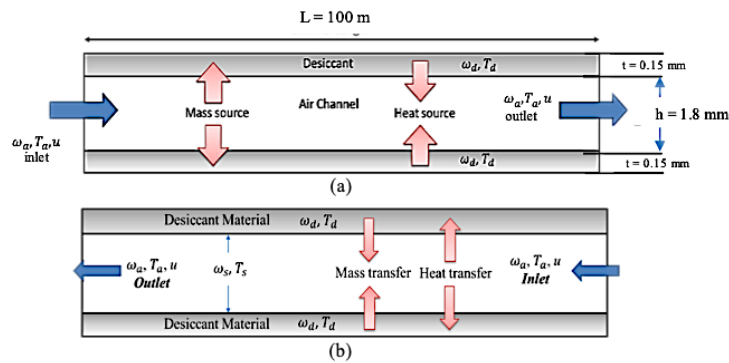


Figure 1 Simplified model of air channel and desiccant layer for: (a) adsorption; and (b) desorption processes

The driving force for the adsorption process is the humidity gradient between the flowing air and the desiccant material. Due to that, the air releases heat and condenses to become water vapor, which falls on the surface of the desiccant material. Desorption is the opposite process of adsorption. During the desorption process, water vapor evaporates into the air because the desiccant material is heated by high-temperature air that flows through the channel. This airflow transports the moist air out of the channel. The numerical simulation was carried out under a transient condition, and the effects of the diffusion of water vapor through the solid desiccant material were neglected. Radiation effects and body forces were negligible. The specific heat and thermal conductivity of the desiccant materials were assumed to be constant. The channel wall

was considered adiabatic. Three desiccant materials were selected for the study purposes, comprising silica gel B, Zeolite 13X, and silica gel-CaCl₂. However, for validating the model, silica gel B was considered for comparison with the experimental data (Zhang et al., 2014). The material properties are listed in Table 1.

Table 1 Thermo-physical properties of desiccant materials (Zhang et al., 2014)

Materials	ρ_d (kg/m ³)	c_d (kJ kg ⁻¹ K)	k_d (k Wm ⁻¹ K)	q_{st} (kJ/kg)	ω_{max} (kg/kg)	ε	C
Silica gel B	790	0.921	1.98×10^{-4}	2362	0.40	0.50	1.1
Silica gel/CaCl ₂	976	0.866	3.20×10^{-4}	2620	0.55	0.41	1.3
Zeolite 13X	650	0.950	2.09×10^{-4}	3843	0.22	0.35	0.2

Figure 2 shows the 3D model of the air channel, which represents the air and desiccant material. Figure 3 shows the front view of the channel. The model was constructed using Multiphysics software. The specifications of the model are based on Zhang et al. (2014). The air domain has one inlet and outlet.

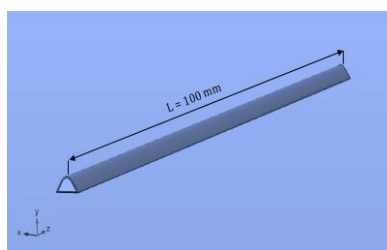


Figure 2 3-D of the air channel

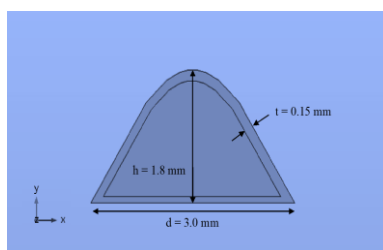


Figure 3 Channel front view

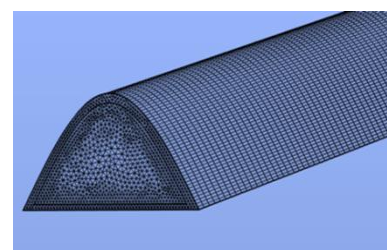


Figure 4 Mesh generation

Three physics models were chosen to solve the above equations, namely the transport of concentrated species, heat transfer in fluid, and convection-diffusion. The geometry was discretized using triangular and prism elements. The elements adjacent to the desiccant material were refined to improve the precision of the numerical solution, as shown in Figure 4. A PARDISO solver and segregated step were used as a solution method and to address each physics model, respectively. The time step was set at 1 second for a total time step of 300.

The numerical model was verified using the grid independent test (GIT). The purpose of this was to establish the number of elements that are able to minimize the effects of meshing on the simulation results. The grid cells were refined for several cases, and the outcomes of the simulation were observed for comparison. Two parameters were analyzed for the GIT, namely air humidity and temperature. Both variables were examined during the adsorption process. The variables were observed along two lines at a vertical plane of the process air outlet.

Line A was located at $x = 1.5$ mm, with Line B at $y = 0.9$ mm. Both the air humidity and temperature solutions along those lines were averaged and compared for subsequent element numbers. Six cases were tested, i.e., 87100, 89100, 126544, 224500, 280625, and 307625. As shown in Figures 5 and 6, it was found that for element number 224500, the air humidity (Figure 5) and temperature (Figure 6) changed insignificantly when compared with the earlier and later cases. However, to minimize computing time during the simulations, element number 280625 was chosen for this study.

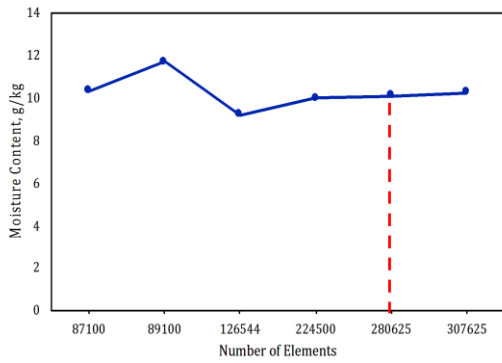


Figure 5 Air humidity with element numbers

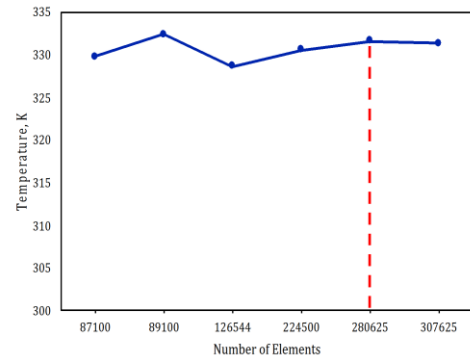


Figure 6 Air temperature with element numbers

3.2. Validation of Numerical Model

The numerical model was validated by comparing the time-variation of average moisture and air temperature at the outlet cross-section of the air channel with the experimental results (Zhang et al., 2014). The inlet boundary conditions are shown in (Table 2). The geometry of the air channel cross-section is honeycomb (sinusoidal), and the desiccant material is silica gel B. The simulation was carried out alternately between the process and regeneration air cycles for the purpose of copying Zhang’s work for three cycles. Each cycle took 300 seconds to complete. The results of the adsorption simulation were then used as the initial conditions for the regeneration process simulation.

Table 2 Inlet conditions of process air

Operating Parameters for process air inlet	Specification	Operating Parameters for regeneration air inlet	Specification
Moisture content, $\omega_{a,inlet}$ (g/kg dry air)	23.25	Moisture content, $\omega_{r,inlet}$ (g/kg dry air)	23.25
Velocity, u (m/s)	1	Velocity, u (m/s)	-1
Temperature, $T_{a, inlet}$ (K)	303	Temperature, $T_{a, inlet}$ (K)	343

Figure 7a shows the variations in the average moisture content (g w.v./kg of d.a.) of air at the outlet of the air channel model (at $z = 100$ mm) during the adsorption process ($t = 0$ to 300 s) and desorption process ($t = 300$ to 600 s) with time. It can be seen that the moisture content of the process air decreases sharply from 23.3 g w.v./kg of d.a. to 13 g w.v./kg of d.a within the first 60 seconds of the adsorption process. The moisture content then increases gradually with time until it reaches 17 g w.v./kg of d.a at the end of the adsorption process. The reason for this trend is that initially, the desiccant material is completely dry and hence, it has a high capacity to remove moisture from the flowing air. However, this ability to remove moisture gradually decreases with time, as more moisture accumulates on its surface. As a result, the process air leaves the channel with increasingly higher humidity. The experimental result reported by Zhang et al. (2014) is also shown for comparison. It can be observed that the result from the numerical simulation follows a similar trend to that of Zhang et al. (2014). At any given time, the moisture content is slightly lower than that of Zhang et al. (2014). The most significant difference of about 3 g w.v./kg of d.a occurs at the time of 60 seconds, while the lowest difference of about 0.5 g w.v./kg of d.a occurs at the time of 300 seconds. One cycle consists of an adsorption process for 300 seconds followed by a desorption process for another 300 seconds. The curve from 300 to 600 seconds represents the variation of moisture content of the regeneration air with time, at the inlet of the air channel model. Note that, during the regeneration process, the inlet of the air

channel (at $z = 0$ mm) becomes the outlet of the regeneration air. During this process, the regeneration air absorbs moisture from the surface of the desiccant material. It can be seen that the moisture content of the regeneration air increases sharply from about 23.25 g w.v./kg of d.a to 29 g w.v./kg of d.a between the times of 300 and 360 seconds. After that, the moisture decreases until it reaches 26 w.v./kg of d.a at the time of 600 seconds. This trend occurs because initially, the regeneration air is completely dry and hence has a high capacity to absorb moisture from the surface of the desiccant material. However, this absorption ability gradually decreases with time as more moisture is absorbed. The simulation result is also compared with that reported by Zhang et al. (2014). It can be observed that at any given time, the simulation result is about 1 g w.v./kg of d.a, which is slightly lower than that reported in the experiment results (Zhang et al., 2014).

Figure 7b shows the variation of the average temperature of process air at the outlet of the air channel model during the adsorption ($t = 0$ to 300 s) and desorption ($t = 300$ to 600 s) processes with time, as obtained from the simulation. It can be seen that during the adsorption process, the air temperature decreases sharply from 353K to 323K within the first 60 seconds. The air temperature then decreases until it reaches 315K at the time of 300 seconds. This is because heat is released from the flowing air during the adsorption process. An experimental result reported by Zhang et al. (2014) is also shown in the figure for comparison. It can be observed that the simulation result has a trend that closely matches that of Zhang et al. (2014). During the desorption process, the process air temperature increases sharply from about 303K to 327K during the first 60 seconds. This is because desiccant material is heated during the regeneration process. As the process air flows over the desiccant material surface, heat is transferred to it. It can also be seen from the figure that, for the next 60 seconds, the air temperature drops slightly. After that, the air temperature increases until it reaches 337K at the time of 600 seconds. The experimental result reported by Zhang et al. (2014) is also shown in the figure for comparison. It can be observed that the variation of process air temperature has a trend similar to that of Zhang et al. (2014). However, at any given time, the simulation result is slightly lower by about 4K compared to the outcome of the experiment results (Zhang et al., 2014).

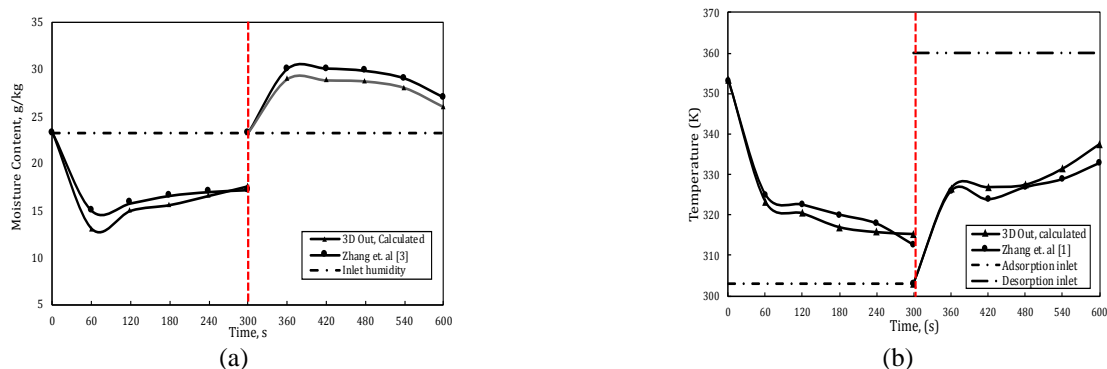


Figure 7 Variations of: (a) moisture content; and (b) process air temperature with time

It can be summarized that the variations of process air humidity and temperature follow similar trends to those reported by Zhang et al. (2014). However, for the adsorption process, the air humidity is about 3.7% lower, and the air temperature is 0.14% lower compared to those of Zhang et al. (2014). For the desorption process, the air humidity is 3.2% lower while the air temperature is 0.01% lower than the results of Zhang et al. (2014). Thus, it would be safe to say that the air channel model is quite well validated and hence can reliably be used for the proceeding simulations.

3.3. Performance of the Desiccant Wheel System

This study aimed to evaluate the performance of the solid desiccant wheel system, namely its MRC, dehumidification effectiveness, and thermal effectiveness. The MRC is given by:

$$MRC = \rho_a u A (\omega_{a,inlet} - \omega_{a,out}) \quad (8)$$

The dehumidification effectiveness, ε_{DW} , and thermal effectiveness, ε_{th} , of the desiccant wheel are given respectively by:

$$\varepsilon_{DW} = \frac{\omega_{a,inlet} - \omega_{a,out}}{\omega_{a,inlet} - \omega_{a,outideal}} \quad (9) \quad \varepsilon_{th} = \frac{T_{a,out} - T_{a,inlet}}{T_{reg} - T_{a,inlet}} \quad (10)$$

4. RESULTS AND DISCUSSION

Figure 8 shows the effects of regeneration temperature on the MRC of different desiccant materials. In this study, the regeneration temperatures were selected to be 40, 50, 60, 70, and 80°C. The three desiccant materials chosen for consideration were silica gel B, Zeolite 13X, and silica gel-CaCl₂. As seen in the figure, MRC increases steadily with the regeneration temperature. This trend was observed for all the desiccant materials considered in this study. This is because, at a higher regeneration temperature, the surface of the desiccant material will be heated to a higher temperature. This provides considerably more thermal energy for the release of moisture from the surface of the desiccant material to the flowing process air. This results in a higher rate of moisture removal. It can also be seen from Figure 8 that at any given regeneration temperature, the MRC of silica gel-CaCl₂ is the highest, while that of zeolite 13X has the lowest value. The MRC of silica gel-CaCl₂ increases from 0.063 g/s at 40°C to 0.067 g/s at 80°C. The MRCs of silica gel B and zeolite 13X also rise, from 0.037 g/s and 0.020 g/s at 40°C to 0.042 g/s and 0.033 g/s at 80°C, respectively.

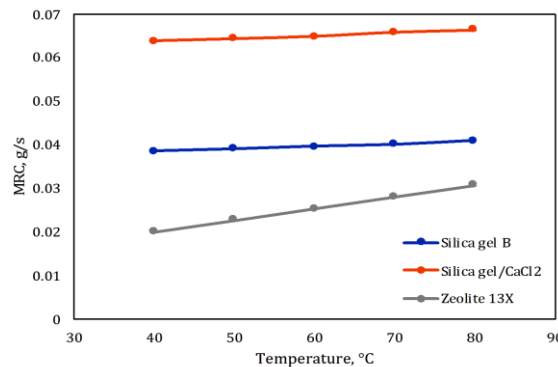


Figure 8 Effects of regeneration temperature on MRC

Figure 9a shows the effects of regeneration temperature on the dehumidification effectiveness of different desiccant materials. Again, it can be observed that the dehumidification effectiveness of all desiccant materials increases with increasing regeneration temperature. The dehumidification effectiveness of silica gel B rises from about 40% at 40°C to 70% at 80°C. The dehumidification effectiveness of Zeolite 13X and silica gel-CaCl₂ increases slightly more steeply, from about 55% and 6% at 40°C to 62% and 20%, respectively, at 80°C.

Figure 9b shows the effects of regeneration temperature on the thermal effectiveness of different desiccant materials. The thermal effectiveness of silica gel-CaCl₂ initially decreases sharply from 53% at 40°C to around 28% at 50°C. It then decreases more gradually to about 15% at 80°C. For Zeolite 13X, it decreases steadily from 25% at 40°C to 5% at 80°C. It can also be noticed from

the figure that, at any given regeneration temperature, silica gel-CaCl₂ has the highest thermal effectiveness while Zeolite 13X has the lowest.

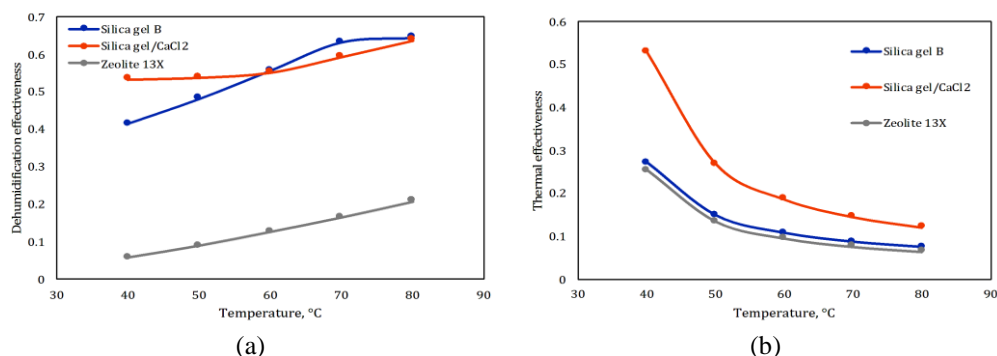


Figure 9 Effects of regeneration air temperature: (a) dehumidification; (b) thermal effectiveness

5. CONCLUSION

A numerical method was used to perform a transient simulation of moisture adsorption and desorption processes in a single air channel of a solid desiccant material. The objective was to determine the MRC, dehumidification effectiveness, and thermal effectiveness of the desiccant material. The numerical model was validated by comparing the variation of air humidity and air temperature at the process air channel outlet with similar data from the literature. For the adsorption process, the relative errors for the air temperature and air humidity were found to be 0.14% and 3.7%, respectively. While for the desorption process, the relative errors for the air temperature and air humidity were 0.01% and 3.2%, respectively. It was also found that at any given regeneration temperature, gel-CaCl₂ has the highest MRC, dehumidification effectiveness, and thermal effectiveness compared to silica gel B and Zeolite 13X.

6. NOMENCLATURE

A	Cross-sectional area of air channel (m ²)	w_{max}	Maximum water uptake of desiccant (kg/kg)
C	Constant in adsorption curve	x	Axial coordinate (m)
c_p	Specific heat (kJ/kg.K)	y	Height coordinate (m)
D_v	Diffusivity (m ² /s)	Greek letters	
D_h	Hydraulic diameter of air channel (m)	φ	Relative humidity
f	Desiccant content	ε_{DW}	Dehumidification effectiveness
h	Convective heat transfer coefficient (kW/m ² .K)	ε_{th}	Thermal effectiveness
k	Convective mass transfer coefficient (m/s)	ε	Porosity
k_m	Internal mass transfer coefficient based on moisture content difference (1/s)	ρ	Density
k_d	Thermal conductivity of desiccant (kW/m.K)	ω	Moisture content
Nu	Nusselt number	Subscript	
q_{st}	Adsorption heat (kJ/kg)	a	Air
Sh	Sherwood number	d	Desiccant
t	Time (s)	ds	Desiccant channel
T	Temperature (K)	eq	Equilibrium
		max	Maximum

7. ACKNOWLEDGEMENT

The authors are grateful to Universiti Teknologi Malaysia for providing the funding for this study, under vote number 20H44. The financial support was managed by the Research Management Centre (RMC), Universiti Teknologi Malaysia.

8. REFERENCES

- Cheng, D., Peters, E., Kuipers, J., 2016. Numerical Modelling of Flow and Coupled Mass and Heat Transfer in an Adsorption Process. *Chemical Engineering Science*, Volume 152, pp. 413–425
- Daou, K., Wang, R., Xia, Z., 2006. Desiccant Cooling Air Conditioning: A Review. *Renewable and Sustainable Energy Reviews*, Volume 10(2), pp. 55–77
- Jia, C., Dai, Y., Wu, J., Wang, R., 2007. Use of Compound Desiccant to Develop High Performance Desiccant Cooling System. *International Journal of Refrigeration*, Volume 30(2), pp. 345–353
- Kamar, H., Kamsah, N., Alhamid, M., Sumeru, K., 2016. Effect of Regeneration Air Temperature on Desiccant Wheel Performance. *International Journal of Technology*, Volume 2, pp. 281–287
- Makaremi, N., Salleh, E., Jaafar, M., GhaffarianHoseini, A., 2012. Thermal Comfort Conditions of Shaded Outdoor Spaces in Hot and Humid Climate of Malaysia. *Building and Environment*, Volume 48, pp. 7–14
- Misha, S., Mat, S., Ruslan, M., Sopian, K., 2012. Review of Solid/Liquid Desiccant in the Drying Applications and its Regeneration Methods. *Renewable and Sustainable Energy Reviews*, Volume 16(7), pp. 4686–4707
- Moncmanová, A., 2007. Environmental Factors that Influence the Deterioration of Materials. *Environmental Deterioration of Materials*, Volume 28, pp. 1–25
- Nguyen, T., Aiello, M., 2013. Energy Intelligent Buildings based on User Activity: A Survey. *Energy and Buildings*, Volume 56, pp. 244–257
- Rambhad, K., Walke, P., Tidke, D., 2016. Solid Desiccant Dehumidification and Regeneration Methods—A Review. *Renewable and Sustainable Energy Reviews*, Volume 59, pp. 73–83
- Satwikasari, A.F., Hakim, L., Prayogi, L., 2018. Enhancing Thermal Environment Quality with Voids and Indoor Gardens as a Passive Design Strategy towards Sustainable and Healthy Living. *International Journal of Technology*, Volume 9(7), pp. 1384–1393
- Sookchaiya, T., Monyakul, V., Thepa, S., 2010. Assessment of the Thermal Environment Effects on Human Comfort and Health for the Development of Novel Air Conditioning System in Tropical Regions. *Energy and Buildings*, Volume 42(10), pp. 1692–1702
- Tharim, A., Munir, F., Samad, M., Mohd, T., 2018. A Field Investigation of Thermal Comfort Parameters in Green Building Index (GBI)-Rated Office Buildings in Malaysia. *International Journal of Technology*, Volume 9(8), pp. 1588–1596
- Wu, D., Wang, R., 2006. Combined Cooling, Heating and Power: A Review. *Progress in Energy and Combustion Science*, Volume 32(5–6), pp. 459–495
- Yadav, L., Yadav, A., Dabra, V., Yadav, A., 2014. Effect of Desiccant Isotherm on the Design Parameters of Desiccant Wheel. *Heat and Mass Transfer*, Volume 50(1), pp. 1–12
- Yamaguchi, S., Saito, K., 2013. Numerical and Experimental Performance Analysis of Rotary Desiccant Wheels. *International Journal of Heat and Mass Transfer*, Volume 60, pp. 51–60
- Yang, W., Zhang, G., 2008. Thermal Comfort in Naturally Ventilated and Air-conditioned Buildings in Humid Subtropical Climate Zone in China. *International Journal of Biometeorology*, Volume 52(5), pp. 385–398
- Zhang, L., Fu, H., Yang, Q., Xu, J., 2014. Performance Comparisons of Honeycomb-type Adsorbent Beds (Wheels) for Air Dehumidification with Various Desiccant Wall Materials. *Energy*, Volume 65, pp. 430–440